

Impact of Doping and Defects on Thermal Transport of Monolayer GaN Nanoribbons: A Molecular Dynamics Simulation Study

1st Md Zesun Ahmed Mia
Electrical Engineering
Pennsylvania State University
State College, Pennsylvania, USA
zesun.ahmed@psu.edu

2nd Nazmus Saadat As-Saqib
Electrical and Computer Engineering
Texas A&M University
College Station, Texas, USA
saadatsaqib@tamu.edu

3rd Mehedi Hasan Himel
Electrical and Computer Engineering
University of Southern California
Los Angeles, California, USA
mehedih713@gmail.com

4th Mehedi Hossen Limon
Electrical and Electronic Engineering
Bangladesh University of Engineering and Technology
Dhaka, Bangladesh
mhlimon1995@gmail.com

5th Samia Subrina
Electrical and Electronic Engineering
Bangladesh University of Engineering and Technology
Dhaka, Bangladesh
samiasubrina@eee.buet.ac.bd

Abstract—Monolayer gallium nitride (GaN), with its graphene-like honeycomb structure, has emerged as a promising material for nanoelectronics and optoelectronic applications. In this study, Equilibrium Molecular Dynamics (EMD) simulations using the Stillinger-Weber (SW) potential were employed to investigate the impact of doping as well as defects on the thermal conductivity of monolayer zigzag GaN nanoribbon (GaN-NR). The thermal transport in aluminum (Al) and indium (In) doped GaN-NR is explored, considering the substitution of both Ga and nitrogen (N) atoms by the dopants. Ga replacement with In led to an increase in thermal conductivity from 11.51 W/m-K to 15.12 W/m-K at a 1% doping concentration. However, in all other cases, whether replacing Ga or N with Al or replacing N with In, it shows an opposite trend, i.e., the thermal conductivity decreases. Furthermore, defects lead to a substantial reduction in thermal conductivity, with a decrease ranging from 68.9% to 77.4% observed at a 2% vacancy concentration across various defect shapes, from point vacancies to hexagon vacancies. We further examine the effect of defect concentrations and defect types on its thermal transport. The results provide valuable insights into the tunability of thermal conductivity in GaN nanostructures, illuminating future optimization for applications in optoelectronic and thermoelectric devices.

Index Terms—GaN Nanoribbon, Molecular Dynamics, Thermal Conductivity, Doping, Defects.

I. INTRODUCTION

Since the discovery of graphene, two-dimensional (2D) materials have attracted considerable attention due to their unique properties [1]. Several 2D materials, such as hexagonal boron nitride (h-BN) [2], silicene [3], molybdenum disulphide [4], phosphorene [5], and borophene [6] have been fabricated and studied. Recently, monolayer gallium nitride (GaN) was synthesized via graphene encapsulation [7]. GaN, like other III-V semiconductors, has applications in electronics and optoelectronics, including HEMTs, LASERs, LEDs, and solar cells

[8]. Studies on GaN monolayers have explored band structures, electronic properties, and tunable bandgaps [9].

With device miniaturization, efficient heat dissipation becomes crucial, making thermal characterization of GaN essential. Qin *et al.* reported a thermal conductivity of 14.93 W/m-K for monolayer GaN using the Boltzmann transport equation (BTE) [9], while Sarma *et. al.* predicted the thermal conductivity of the monolayer GaN nanosheet to be 25 W/m-K at 300K with equilibrium Green-Kubo (GK) formulations [10]. Jiang *et al.* found 37 W/m-K for hexagonal GaN and 9.3 W/m-K for its haecelite form [11], much lower than graphene (3094.03 W/m-K) [12] and bulk GaN (310 to 380 W/m-K) [13]. Further studies have investigated the effects of electric fields on the phonon transport and the thermal conductivity of GaN [14].

Structural modifications in materials can be engineered through doping and the creation of vacancies. In binary compounds like GaN, BN, and MoSe₂, doping involves substituting atoms, such as replacing Mo or Se in MoSe₂ with dopant atoms, which alters thermal conductivity, electronic properties, and mechanical stability [15]. Previous studies show that aluminum and indium effectively modulate the thermal and electronic behaviors of thin film GaN [16]. Defects like vacancies are often formed unintentionally during synthesis or can be intentionally engineered to tailor material properties [17]. In 2D materials, such as graphene and h-BN, vacancies significantly reduce thermal conductivity [18]. In monolayer GaN, point defects like Ga and N vacancies affect structural, electrical, and magnetic properties, including lattice constants and bandgaps [19]. Complex multi-atom vacancies, such as triangular and hexagonal types, are increasingly explored for their role in tuning 2D material properties [20].

Noshin *et al.* demonstrated the significant reduction in

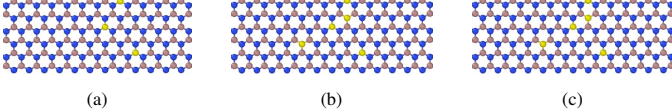


Fig. 1: Schematic diagram of 15 nm x 4 nm doped monolayer GaN nanoribbon. Ga and N atoms are represented by brown and blue colored spheres respectively. Yellow spheres represent the dopant atoms (Al or In). Dopant atom replaces (a) Ga atoms (b) N atoms (c) both Ga and N atoms.

thermal conductivity due to vacancies in graphene nanoribbons [21]. Hassan *et al.* focused on the electronic and optical properties of doped GaN [22]. Hossain *et al.* studied thermal transport in monolayer pristine and defected GaN using non-equilibrium molecular dynamics (NEMD) simulations [23]. Similarly, Sun *et al.* emphasized higher-order phonon scattering in 2D-GaN but did not explore how vacancy defects affect its thermal conductivity [24]. However, detailed investigations of the effects of doping and complex vacancy types on thermal transport in 2D-GaN are yet to be explored. In this work, we conduct a thorough study of thermal transport in monolayer gallium nitride nanoribbon (GaN-NR) with various doping concentrations and complex vacancies using equilibrium molecular dynamics simulations with the Stillinger-Weber potential [25]. First, we investigate the thermal conductivity of pristine GaN-NR. We then explore the effects of various doping concentrations, particularly with Group III elements such as aluminum and indium, on the thermal properties of GaN-NR. Additionally, the impact of defects, including different types of vacancies such as point and bi-vacancies, as well as multi-atom vacancies like triangle, rhombus, pentagon, and hexagon vacancies is systematically examined. This study provides comprehensive insights into how doping and vacancy engineering affect the thermal conductivity of GaN-NR, offering valuable data for optimizing thermal transport in this material and giving a crucial understanding of its use in thermal management and thermoelectric applications.

II. SIMULATION DETAILS

Equilibrium Molecular Dynamics simulations for the system were performed in LAMMPS [26]. The non-buckled honeycomb GaN nanoribbon structure, with a Ga-N bond length of 1.88 Å [27] and a lattice parameter of 3.21 Å. Wang *et al.* demonstrated that the non-buckled GaN structure is more stable than the buckled counterpart due to its lower formation energy [27]. The pristine GaN-NR is of size 15 nm × 4 nm with a thickness of 3.74 Å, as reported by Qin *et al.* [9], has been studied in this work. We also investigate the thermal conductivity of doped GaN-NR, using aluminum and indium as dopants [28]. The doping process involves substituting Ga, N, or both atoms with dopant atoms, as illustrated in Fig. 1. To analyze the impact of defects, structures with various vacancies, shown in Fig. 2a to Fig. 2f, were simulated. Fig. 2a displays single-atom vacancies, while Fig. 2b to Fig. 2f represent multi-atomic defects, including bi-atomic, triangular, rhombus, pentagonal, and hexagonal vacancies, with defect locations randomly distributed across the nanoribbon.

The interactions between atoms were modeled using the Stillinger-Weber (SW) potential, parameterized by Bere and

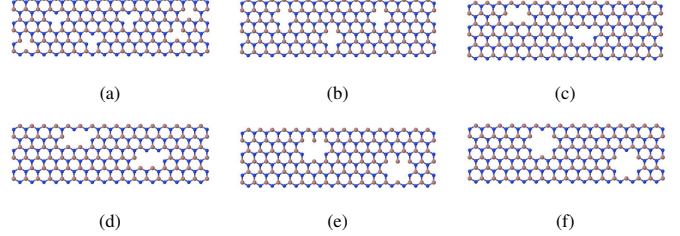


Fig. 2: Schematic representation of a 15 nm x 4 nm monolayer GaN nanoribbon used to study thermal transport, along with different vacancy structures to simulate the effect of defects on thermal conductivity: (a) point vacancy, (b) bi-vacancy, (c) triangle vacancy, (d) rhombus vacancy, (e) pentagon vacancy, and (f) hexagon vacancy.

Serra for hexagonal structures [25]. For Al- and In-doped GaN nanoribbons, the SW potential parameterized by Zhou *et al.* was employed [29]. A 3-body potential was used to account for all types of interactions between atoms. Thermal conductivity was calculated using Equilibrium Molecular Dynamics (EMD) simulations, based on the Green-Kubo formulation, which integrates the ensemble average of the heat current autocorrelation function (HCACF). The Green-Kubo formula is provided in Eqn. 1

$$K_x = \frac{1}{V K_B T^2} \int_0^\tau \langle J_x(t) \cdot J_x(0) \rangle dt \quad (1)$$

here, K_x is the thermal conductivity in the x direction, V is the system volume defined as the area of the monolayer structure multiplied with the van der Waals thickness, K_B is the Boltzmann constant, T is temperature of the system, τ is required correlation time for the decay of HCACF reasonably close to zero. $\langle J_x(t) \cdot J_x(0) \rangle$ is the ensemble averaging term, which can be calculated from the heat current Eqn. 2.

$$J(t) = \sum_i \epsilon_i v_i + \frac{1}{2} \sum_{ij} (F_{ij}, v_i) r_{ij} \quad (2)$$

where ϵ_i is the total site energy, v_i is the time-dependent velocity of atom i , $r_{ij} = r_i - r_j$ (r_i is the time-dependent position of atom i), and F_{ij} is the force exerted by atom j on atom i . In our study, thermal conductivity was computed using molecular dynamics simulations with periodic boundary conditions applied in all directions. A fixed time step of 0.5 fs was used, with thermal equilibration achieved via the Nose-Hoover thermostat over 2×10^5 steps, followed by an NVE ensemble for 2×10^6 steps. Energy minimization was done using the steepest descent algorithm and the Velocity-Verlet integrator [30] was employed to integrate Newton's equations of motion. In-plane heat current data were recorded every five steps and the heat current autocorrelation function (HCACF) was averaged over ten samples. The thermal conductivity was calculated using these HCACF values and averaged over five independent NVE ensembles, each with a different initial condition. For phonon density of states (PDOS) calculations, the *FixPhonon* command in LAMMPS was used to extract dynamical matrices, followed by post-processing with *phana* [31]. PDOS convergence was ensured using a 24 x 24 x 1 mesh grid after testing various densities.

III. RESULTS AND DISCUSSION

The calculated room temperature (300K) thermal conductivity of 15 nm × 4 nm zigzag monolayer gallium nitride using

Stillinger-Weber potential is 11.5 ± 0.408 W/m-k [9], [32]. Qin *et. al.* showed that in monolayer GaN, the phonon-phonon scattering is dominated by the Umklapp scattering process, while for graphene and monolayer boron nitride Normal scattering process dominates the phonon-phonon scattering. This causes a significant lowering of thermal conductivity in monolayer GaN. Additionally, the planar honeycomb structure of monolayer GaN is not as perfectly smooth as that of graphene due to a large difference in atomic radii (the atomic radius of Ga is almost twofold of that of N), leading to slightly broken phonon-phonon selection rule and relatively lower contribution of flexural phonon in monolayer GaN [9]. Furthermore, it is well known that the phonon-phonon scattering process is determined by the anharmonic nature of structures, whose magnitude can be roughly quantified by the Grüneisen parameter (γ). The magnitude of γ for monolayer GaN is obviously larger than silicene, meaning stronger phonon anharmonicity in monolayer GaN. The strong phonon-phonon scattering due to the anharmonicity leads to the small phonon lifetime of monolayer GaN, and thus leads to the low thermal conductivity of monolayer GaN. Another insightful concept arises from charge transfer between N (electronic charge = 5.527) and Ga (electronic charge = 2.473) atoms which results in the strongly polarized covalent bonds in monolayer GaN due to a significant difference in electronegativity (1.81 for Ga and 3.0 for N) [33]. This inhomogeneous distribution of charge density in monolayer GaN induces additional long-range electrostatic Coulomb forces on atoms and makes atoms much more restrained when oscillating around the equilibrium position. This leads to stronger intrinsic phonon-phonon scattering and further contributes to lower thermal conductivity.

A. Effect of Doping

To investigate the impact of doping on the thermal conductivity of monolayer GaN nanoribbons (GaN-NRs), the structures depicted in Fig. 1 were utilized in the simulation. Fig. 3 illustrates the variation in thermal conductivity of monolayer GaN-NR at room temperature (300K) across different doping concentrations. The doping level ranges from 0.5% to 2% of the total atoms in the monolayer GaN-NR. In general, the doped GaN-NR exhibits lower thermal conductivity compared to its pristine form, with the exception of indium doping replacing gallium atoms. Additionally, for all doping configurations, the thermal conductivity shows a decreasing trend as the concentration of aluminum or indium atoms increases.

The thermal transport in Al-doped monolayer GaN-NR can be explained by considering the phonon density of states (PDOS) for the pristine and Al-doped monolayer GaN-NR. The PDOS curves for Ga-substitution and N-substitution by Al are depicted in Fig. 4a and Fig. 4b, respectively. As shown in Fig. 4a, Ga-substitution causes a red shift of the high-frequency peaks compared to pristine monolayer GaN-NR (from ~ 21 Hz to $\sim 15\text{-}19$ Hz). The Al-doped GaN-NR also exhibits softened high-frequency peaks, indicating fewer phonons for thermal transport and hence lower thermal conductivity. Furthermore, the Al-doped monolayer GaN-NR

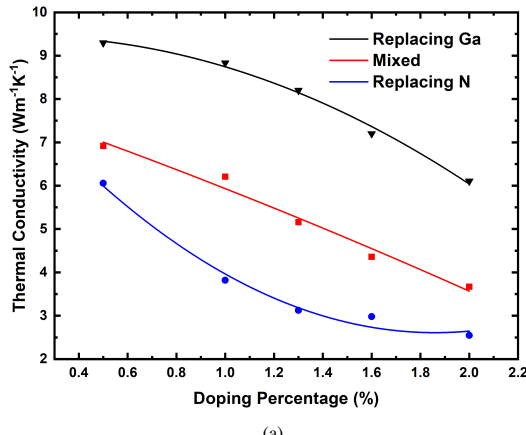
shows higher peaks in the lower frequency range compared to the pristine material, which indicates a larger number of phonons in this region, causing shortening of mean free path and reduction in phonon lifetime. This leads to further reduction in thermal conductivity. For N-substitution by Al (Fig. 4b), the red shift in high-frequency peaks is more significant, shifting phonons to lower frequencies (from ~ 21 Hz to ~ 13 Hz), shortening their mean free path and lifetime, and increasing scattering, which results in a further reduction in thermal conductivity. In mixed doping, where both Ga and N are replaced by Al, thermal conductivity falls between that of the individual Ga- and N-substituted cases, as shown in Fig. 3a.

A decreasing trend of thermal conductivity with increasing doping concentration is shown in Fig. 3b, where In-doped monolayer GaN-NR exhibits greater thermal conductivity in the case of Ga-substitution and lower thermal conductivity in the case of N-substitution compared to pristine monolayer GaN. This behavior of In-doped GaN can be understood through the concept of mass variance, which significantly influences phonon scattering mechanisms. Hahn *et. al.* demonstrated the impact of doping on thermal conductivity and highlighted the critical role of mass variance in phonon scattering mechanisms. Mass variance (var_m) in a ternary system is expressed by [34]:

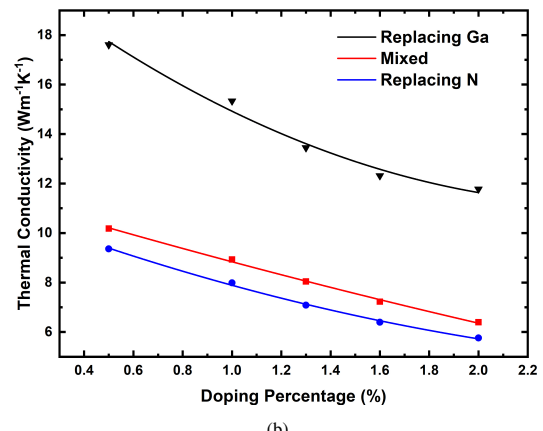
$$\text{var}_m = \frac{(m_1 - m_k)^2}{m_k^2} + \frac{(m_2 - m_k)^2}{m_k^2}$$

where m_k is the atomic mass of the dopant, and m_1 and m_2 are the atomic masses of the host materials. Their analysis included various doping elements such as nitrogen (N), phosphorus (P), arsenic (As), boron (B), aluminum (Al), and gallium (Ga), demonstrating that the impact of doping on thermal conductivity varies depending on the atomic mass of the dopant relative to the host materials. For example, Al doping in SiGe exhibited a mass variance of approximately 2.87, resulting in a significant decrease in thermal conductivity, while doping with As, which had a lower mass variance of 0.39, led to an increase in thermal conductivity due to reduced phonon scattering. Similarly, doping with B and P also decreased thermal conductivity, while doping with Ga increased it.

In the case of In and Al doping in monolayer GaN nanoribbons, In, with an atomic mass of 114.8 amu, is heavier than aluminum (27.0 amu) but only 1.6 times the mass of gallium (69.7 amu). When Al, which is 2.6 times lighter than Ga, replaces Ga, it introduces scattering centers for phonons responsible for heat transport. The mass variance for Al doping is approximately 2.73, suggesting significant phonon scattering and reduction in thermal conductivity, while the mass variance for In doping is around 0.96, indicating limited phonon scattering and enhanced thermal conductivity. Thus, the interplay between atomic mass and substitution effects in GaN nanoribbons mirrors the trends observed in the doping of SiGe alloys [34], where mass variance directly correlates with thermal conductivity changes. Additionally, the heat current autocorrelation function (HCACF) depicted in Fig. 5 shows

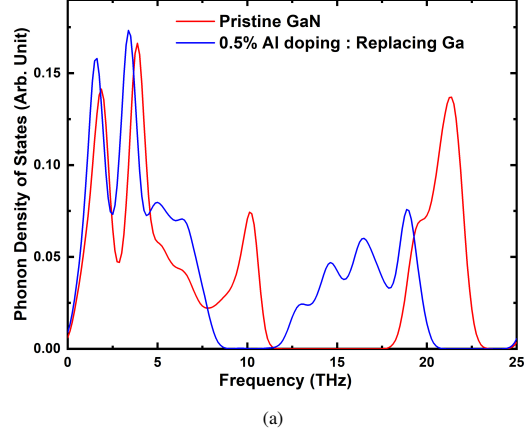


(a)

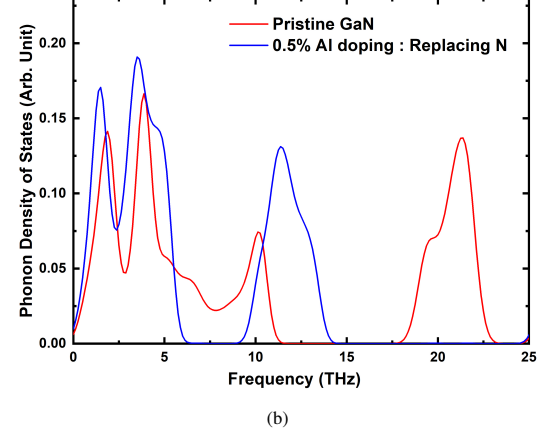


(b)

Fig. 3: Variation of thermal conductivity of doped monolayer GaN nanoribbon with respect to doping percentage, when doped with (a) aluminum atoms and (b) indium atoms.



(a)



(b)

Fig. 4: Phonon density of states (PDOS) of monolayer GaN-NR doped with aluminum, where (a) Ga atoms and (b) N atoms are replaced by Al atoms.

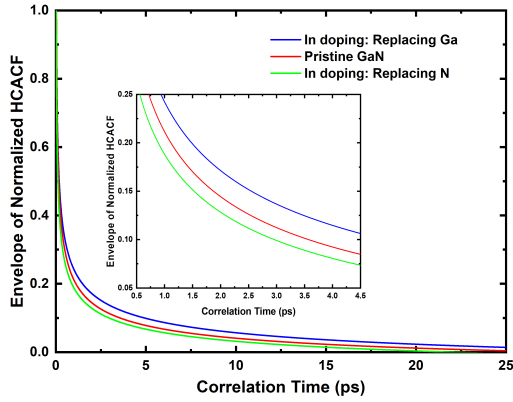


Fig. 5: HCACF of In-doped and undoped samples of monolayer GaN-NR showing the relaxation times of each of the samples indicating the variety in thermal conductivity; magnified view is shown in the inset.

that the HCACF decay is most relaxed for In doping in place of Ga, indicating the highest thermal conductivity in this scenario. However, as doping concentration increases, impurity centers in the nanoribbon also increase, leading to enhanced phonon impurity scattering, which ultimately reduces thermal conductivity. This aligns with the findings of Zhequan Yan et. al., who reported that doping with tungsten in monolayer MoSe₂ can enhance thermal conductivity beyond that of the pristine structure [35]. Additionally, Hassan et. al.

demonstrated how the mass of dopants and their interactions with host atoms influence the overall thermal conductivity of the system [32]. Liang et. al. also highlighted the role of doping concentration, showing that the thermal conductivity of Si nanowires initially decreases before increasing with higher Ge concentration [36]. This indicates that the variation in thermal conductivity, as well as its magnitude, is influenced by several factors, including dopant mass, mass variance relative to host atoms, their interactions, and doping concentration. It is essential to understand these complex relationships for optimizing the thermal properties of doped materials and advancing their applications in semiconductor technology.

B. Effect of Vacancies

To investigate the effects of various types of vacancies on the thermal conductivity of monolayer GaN-NR, different types of defects, that is, vacancies, are created and defect concentrations are varied. Fig. 6a shows the thermal conductivity of a 15 nm × 4 nm monolayer GaN as a function of defect percentage for point vacancies. The results indicate how thermal conductivity is influenced by the type of vacancy and its concentration. For all types of vacancies, a similar trend is observed where thermal conductivity decreases with increasing defect concentration (vacancy percentage) as seen in graphene nanoribbons (GNR) and hexagonal boron nitride nanoribbons (h-BNNR) in the presence of defects. [37]. However, the rate

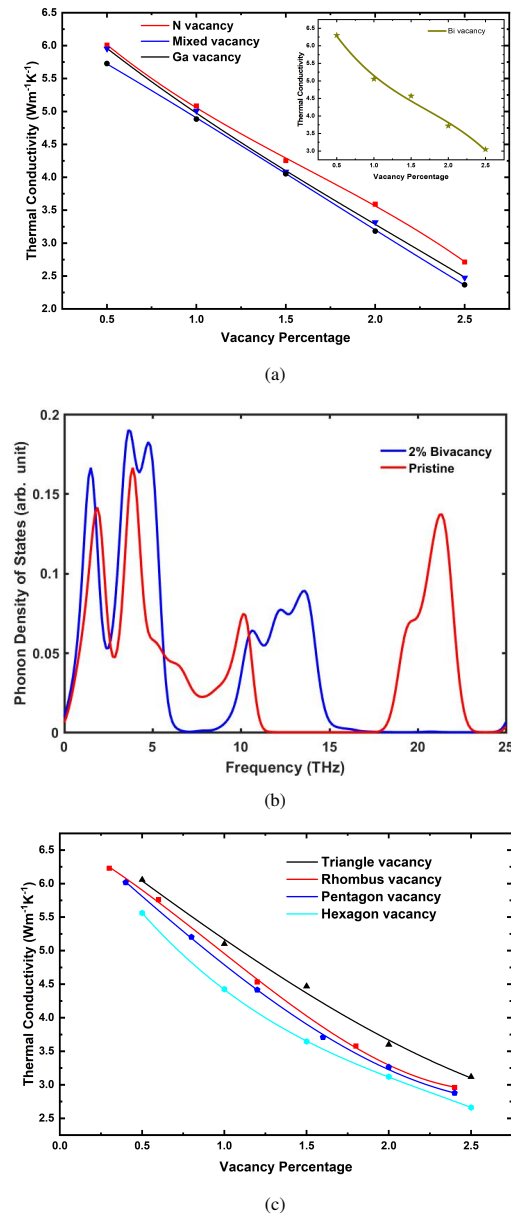


Fig. 6: (a) Thermal conductivity variation for point vacancies (inset: bi-vacancies), (b) phonon density of states comparing bi-vacancies with pristine GaN, and (c) thermal conductivity variation for geometric pattern vacancies.

of decay varies with the type of vacancy. In the case of point vacancies, the breaking of sp^2 bonds amplifies phonon scattering, which negatively impacts the thermal conductivity of monolayer GaN [9], [38]. Point vacancies for three distinct cases—Ga vacancies, N vacancies, and mixed vacancies (both Ga and N)—show different thermal conductivities, as depicted in Fig. 6a. The data suggest that nitrogen vacancies have a smaller impact on thermal conductivity than gallium vacancies due to the differences in atomic mass and size [3].

Manufacturing constraints often lead to defects in synthesized monolayers like h-BN and h-GaN, making it difficult to achieve defect-free structures [39]. Additionally, tuning the thermal conductivity of monolayer GaN may be necessary for specific applications, and this can be accomplished through

the controlled introduction of vacancies. Beyond simple point vacancies, more complex geometric pattern vacancies—such as bi, triangular, rhombus, pentagonal, and hexagonal vacancies—offer further potential for tuning thermal properties. Fig. 6c illustrates the effect of various geometric vacancies on the thermal conductivity of monolayer GaN-NR. The impact of these vacancies depends on the shape of the dislocation center. Bi-vacancies do not reduce the thermal conductivity as much as point vacancies. The partial restoration of sp^2 bonds in bi-vacancies helps mitigate the reduction in thermal conductivity, resulting in less phonon scattering compared to other vacancy types [38]. Fig. 6b shows the thermal conductivity reduction relative to pristine GaN-NR, evidenced by the shift and amplitude reduction of the high-frequency peak in the phonon density of states (PDOS) for GaN with 2% bi-vacancy. As the amplitude of the high-frequency peak decreases, the number of phonons available for thermal transport declines, leading to reduced thermal conductivity. As the shape pattern of the vacancy increases from triangular vacancies to hexagonal vacancies, phonon mean free paths are shortened, leading to more pronounced scattering and thus a larger reduction in thermal conductivity. These geometric pattern vacancies partially restore sp^2 bonds; however, the scattering effect caused by the size of the dislocation center outweighs this, leading to a reduction in thermal conductivity compared to bi-vacancies. Each type of pattern vacancy produces distinct effects. For example, triangular vacancies, with their smaller dislocation center, introduce less scattering compared to larger vacancies. As a result, the thermal conductivity for a given defect concentration is highest in the case of triangular vacancies among the geometric patterns and progressively decreases as the vacancy shape becomes more complex, with hexagonal vacancies having the largest scattering effects (Fig. 6c). Larger vacancy types disrupt the lattice more significantly, reducing the mean free path of phonons and contributing to increased thermal resistance. This behavior underscores the importance of vacancy engineering in optimizing the thermal properties of 2D materials like GaN, where specific patterns of vacancies can be introduced to achieve targeted thermal performance for applications such as thermoelectrics or heat management in nanoscale devices.

IV. CONCLUSION

In this study, we have investigated the thermal conductivity of monolayer gallium nitride nanoribbons (GaN-NR), focusing on the impact of doping and defects. We observe that thermal conductivity consistently decreases as doping concentration increases, nitrogen substitution results in lower conductivity than gallium substitution for both Al and In doping. Notably, In doping at Ga sites increases thermal conductivity, while Al doping reduces it. Defects, particularly vacancies, drastically lower the thermal conductivity of GaN-NR, with dislocations causing more phonon scattering. Different geometric pattern vacancies allow precise control over thermal properties, providing flexibility in tailoring the thermal conductivity of GaN-NR for specific applications. Moreover, the structures exhibit

good thermal stability, making them suitable for thermoelectric, nanoelectronic, and optoelectronic devices.

REFERENCES

- [1] K. S. Novoselov, "Electric field effect in atomically thin Carbon films," *Science*, vol. 306, no. 5696, p. 666–669, Oct 2004.
- [2] N. G. Chopra, R. Luyken, K. Cherrey, V. H. Crespi, M. L. Cohen, S. G. Louie, and A. Zettl, "Boron Nitride Nanotubes," *Science*, vol. 269, no. 5226, pp. 966–967, 1995.
- [3] P. Vogt, P. De Padova, C. Quaresima, J. Avila, E. Frantzeskakis, M. C. Asensio, A. Resta, B. Ealet, and G. Le Lay, "Silicene: compelling experimental evidence for Graphene-like two-dimensional Silicon," *Phys. Rev. Lett.*, vol. 108, p. 155501, Apr 2012. [Online]. Available: <https://link.aps.org/doi/10.1103/PhysRevLett.108.155501>
- [4] K. S. Novoselov, A. K. Geim, S. V. Morozov, D. Jiang, M. I. Katsnelson, I. V. Grigorieva, S. V. Dubonos, and A. A. Firsov, "Two-dimensional gas of massless Dirac Fermions in Graphene," *Nature*, vol. 438, no. 7065, p. 197–200, Nov 2005.
- [5] L. Li, Y. Yu, G. J. Ye, Q. Ge, X. Ou, H. Wu, D. Feng, X. H. Chen, and Y. Zhang, "Black Phosphorus field-effect transistors," *Nature nanotechnology*, vol. 9, no. 5, p. 372, 2014.
- [6] A. J. Mannix, X.-F. Zhou, B. Kiraly, J. D. Wood, D. Alducin, B. D. Myers, X. Liu, B. L. Fisher, U. Santiago, J. R. Guest *et al.*, "Synthesis of Borophenes: anisotropic, two-dimensional Boron polymorphs," *Science*, vol. 350, no. 6267, pp. 1513–1516, 2015.
- [7] Z. Y. Al Balushi, K. Wang, R. K. Ghosh, R. A. Vilá, S. M. Eichfeld, J. D. Caldwell, X. Qin, Y.-C. Lin, P. A. DeSario, G. Stone *et al.*, "Two-dimensional Gallium Nitride realized via Graphene encapsulation," *Nature materials*, vol. 15, no. 11, pp. 1166–1171, 2016.
- [8] H.-M. Kim, Y.-H. Cho, H. Lee, S. I. Kim, S. R. Ryu, D. Y. Kim, T. W. Kang, and K. S. Chung, "High-brightness light emitting diodes using dislocation-free Indium Gallium nitride/Gallium Nitride multiquantum-well nanorod arrays," *Nano letters*, vol. 4, no. 6, pp. 1059–1062, 2004.
- [9] Z. Qin, G. Qin, X. Zuo, Z. Xiong, and M. Hu, "Orbitally driven low thermal conductivity of monolayer Gallium Nitride (GaN) with planar honeycomb structure: a comparative study," *Nanoscale*, vol. 9, no. 12, pp. 4295–4309, 2017.
- [10] J. V. N. Sarma, R. Chowdhury, and R. Jayaganthan, "Molecular dynamics investigation of the thermomechanical behavior of monolayer Gallium Nitride (GaN)," *Journal of Applied Physics*, vol. 113, no. 24, p. 243504, Jun 2013.
- [11] Y. Jiang, S. Cai, Y. Tao, Z. Wei, K. Bi, and Y. Chen, "Phonon transport properties of bulk and monolayer Gallium Nitride (GaN) from first-principles calculations," *Computational Materials Science*, vol. 138, pp. 419–425, 2017.
- [12] S. J. Mahdizadeh and E. K. Goharshadi, "Thermal conductivity and heat transport properties of Graphene nanoribbons," *Journal of nanoparticle research*, vol. 16, no. 8, pp. 1–12, 2014.
- [13] T. Kawamura, Y. Kangawa, and K. Kakimoto, "Investigation of thermal conductivity of Gallium Nitride (GaN) by molecular dynamics," *Journal of crystal growth*, vol. 284, no. 1-2, pp. 197–202, 2005.
- [14] Y. Quan, S.-Y. Yue, and B. Liao, "Electric field effect on the thermal conductivity of wurtzite gan," *Applied Physics Letters*, vol. 118, no. 16, p. 162110, 2021.
- [15] Z. Yan, M. Yoon, and S. Kumar, "Influence of defects and doping on phonon transport properties of monolayer Molybdenum Diselenide," *2D Materials*, vol. 5, no. 3, p. 031008, 2018.
- [16] A. Filatova-Zalewska, Z. Litwicki, T. Suski, and A. Jeżowski, "Thermal conductivity of thin films of Gallium Nitride, doped with Aluminium, measured with 3ω method," *Solid State Sciences*, vol. 101, p. 106105, 2020.
- [17] G. Ye, Y. Gong, J. Lin, B. Li, Y. He, S. T. Pantelides, W. Zhou, R. Vajtai, and P. M. Ajayan, "Defects engineered monolayer Molybdenum Disulfide for improved Hydrogen evolution reaction," *Nano letters*, vol. 16, no. 2, pp. 1097–1103, 2016.
- [18] X. Wu and Q. Han, "Thermal conductivity of monolayer hexagonal Boron Nitride: From defective to amorphous," *Computational Materials Science*, vol. 184, p. 109938, 2020.
- [19] K. H. Yeoh, K.-H. Chew, T. L. Yoon, Rusi, and D. Ong, "Strain-tunable electronic and magnetic properties of two-dimensional Gallium Nitride with vacancy defects," *Journal of Applied Physics*, vol. 127, no. 1, p. 015305, 2020.
- [20] L.-S. Zhao, C.-P. Chen, L.-L. Liu, H.-X. Yu, Y. Chen, and X.-C. Wang, "Magnetism and piezoelectricity of hexagonal Boron Nitride with triangular vacancy," *Chinese Physics B*, vol. 27, no. 1, p. 016301, 2018.
- [21] M. Noshin, A. I. Khan, I. A. Navid, H. A. Uddin, and S. Subrina, "Impact of vacancies on the thermal conductivity of Graphene nanoribbons: A molecular dynamics simulation study," *AIP Advances*, vol. 7, no. 1, p. 015112, 2017.
- [22] M. Hassan, F. Rahman, M. Islam, and T. Hossain, "Structural, electronic and optical characterization of edge passivated B and P doped Gallium Nitride (GaN) nanostructures," *Journal of Applied Physics*, vol. 131, no. 7, p. 074501, 2022.
- [23] A. Hossain, A. J. Islam, K. B. Zaman, and M. R. Islam, "Thermal Transport Behavior of Monolayer Gallium Nitride: A Non-equilibrium Molecular Dynamics Study," in *6th International Conference on Electrical Information and Communication Technology (EICT)*. IEEE, 2023, pp. 1–5.
- [24] J. Sun, X. Liu, Y. Xiong, Y. Yao, X. Yang, C. Shao, and S. Li, "Revisiting phonon thermal transport in two-dimensional Gallium Nitride: Higher-order phonon-phonon and phonon-electron scattering," *Journal of Applied Physics*, vol. 132, p. 034508, 2024.
- [25] A. Bére and A. Serra, "On the atomic structures, mobility and interactions of extended defects in Gallium Nitride (GaN) : dislocations, tilt and twin boundaries," *Philosophical Magazine*, vol. 86, no. 15, pp. 2159–2192, 2006.
- [26] S. Plimpton, "Fast parallel algorithms for short-range molecular dynamics," *Journal of computational physics*, vol. 117, no. 1, pp. 1–19, 1995.
- [27] V. Wang, Z. Wu, Y. Kawazoe, and W. Geng, "Tunable Band Gaps of In x Ga $1-x$ N Alloys: From Bulk to Two-Dimensional Limit," *The Journal of Physical Chemistry C*, vol. 122, no. 12, pp. 6930–6942, 2018.
- [28] L. Zhao, H. Chang, W. Zhao, Z. Luan, X. Tian, C. Tan, and Y. Huang, "Coexistence of doping and strain to tune electronic and optical properties of Gallium Nitride (GaN) monolayer," *Superlattices and Microstructures*, vol. 130, pp. 93–102, 2019.
- [29] X. W. Zhou, R. E. Jones, and K. Chu, "Polymorphic improvement of Stillinger-Weber potential for InGaN," *Journal of Applied Physics*, vol. 122, no. 23, p. 235703, 2017.
- [30] D. L. Cheung, L. Anton, M. P. Allen, and A. J. Masters, "Computer simulation of liquids and liquid crystals," *Computer Physics Communications*, vol. 179, no. 1-3, pp. 61–65, 2008.
- [31] L. T. Kong, "Phonon dispersion measured directly from molecular dynamics simulations," *Computer Physics Communications*, vol. 182, no. 10, pp. 2201–2207, 2011.
- [32] M. A. Hassan and S. Subrina, "Thermal transport characterization of monolayer GaN nanoribbon doped with group IV materials: An equilibrium molecular dynamics study," *Materials Today Communications*, vol. 38, p. 108532, 2024. [Online]. Available: <https://www.sciencedirect.com/science/article/pii/S2352492824005129>
- [33] D. C. Camacho-Mojica and F. López-Urías, "GaN haeckelite single-layered nanostructures: monolayer and nanotubes," *Scientific reports*, vol. 5, no. 1, pp. 1–11, 2015.
- [34] K. R. Hahn, C. Melis, F. Bernardini, and L. Colombo, "Engineering the thermal conductivity of doped SiGe by mass variance: A first-principles proof of concept," *Front. Mech. Eng.*, vol. 7, Jul. 2021.
- [35] Z. Yan, M. Yoon, and S. Kumar, "Influence of defects and doping on phonon transport properties of monolayer Molybdenum Diselenide," *2D Materials*, vol. 5, no. 3, Apr. 2018, publisher Copyright: © 2018 IOP Publishing Ltd.
- [36] Q. Liang, Y.-L. He, and T.-C. Hung, "Manipulating thermal conductivity of Silicon nanowires through surrounded fins and Ge dopant," *International Journal of Heat and Mass Transfer*, vol. 176, p. 121425, 2021. [Online]. Available: <https://www.sciencedirect.com/science/article/pii/S0017931021005287>
- [37] A. I. Khan, I. A. Navid, M. Noshin, H. Uddin, F. F. Hossain, and S. Subrina, "Equilibrium Molecular Dynamics (MD) simulation study of thermal conductivity of Graphene nanoribbon: a comparative study on MD potentials," *Electronics*, vol. 4, no. 4, pp. 1109–1124, 2015.
- [38] M. Imran, F. Hussain, M. Rashid, H. Ullah, A. Sattar, F. Iqbal, and E. Ahmad, "Comparison of Electronic and Optical Properties of Gallium Nitride (GaN) Monolayer and Bulk Structure: a First Principle Study," *Surface Review and Letters*, vol. 23, no. 04, p. 1650026, 2016.
- [39] D. Akinwande, C. J. Brennan, J. S. Bunch, P. Egberts, J. R. Feits, H. Gao, R. Huang, J.-S. Kim, T. Li, Y. Li *et al.*, "A review on mechanics and mechanical properties of 2D materials—Graphene and beyond," *Extreme Mechanics Letters*, vol. 13, pp. 42–77, 2017.